

## Relativistic all-order calculations of energies and matrix elements in cesium

S. A. Blundell,\* W. R. Johnson, and J. Sapirstein

*Department of Physics, University of Notre Dame, Notre Dame, Indiana 46556*

(Received 29 October 1990)

All-order methods recently developed for high-accuracy calculation of energies and matrix elements in Li are extended and applied to cesium. We employ a relativistic, linearized, coupled-cluster formalism, incorporating single, double, and an important subset of triple excitations. A coupled-cluster formulation of the matrix element of a one-body operator, incorporating the random-phase approximation exactly, is used to calculate hyperfine constants and transition-matrix elements. We find agreement with experiment at the 0.5% level or better for ionization energies and dipole-matrix elements, and at the 1% level for hyperfine constants. Modifications of the method that have the potential of higher accuracy are discussed.

### I. INTRODUCTION

Many-body perturbation theory (MBPT) provides a powerful and systematic method of calculating the properties of many-electron systems.<sup>1</sup> However, while consideration of the first few orders of MBPT is known to suffice for accurate calculations of the properties of highly charged ions,<sup>2</sup> the method is less highly convergent for neutral atoms. For this reason, it is of interest to consider methods that sum infinite classes of MBPT diagrams, which we refer to as “all-order” methods. One of the best known of these methods is the coupled-cluster formalism (reviewed by, e.g., Bishop and Kümmel<sup>3</sup>). The majority of applications of this formalism have been made to closed-shell systems in a nonrelativistic framework. Interest in the accurate calculation<sup>4,5</sup> of parity nonconservation in cesium, however, requires a relativistic method because of the high nuclear charge and the short-distance origin of the effect, and in addition a method that deals with an open-shell system, here the simplest possible case of a single electron outside closed shells.

Before carrying out any calculation of parity nonconservation, the strength of which effect depends on an unknown quantity, the so-called weak nuclear charge  $Q_W$ ,<sup>6</sup> it is necessary to calculate known properties of the atom to provide a gauge of the accuracy of the calculation. The accuracy required for extraction of useful information about unified theories of the weak and electromagnetic interactions is on the order of 1%. What we wish to do in this paper is to describe in detail a relativistic, open-shell, all-order method that is powerful enough to predict experimentally known energy levels and matrix elements of cesium to this accuracy. We have already applied the method to the calculation of parity nonconservation in cesium.<sup>4</sup>

Previously we used a relativistic, all-order method to calculate energies and matrix elements for Li and  $\text{Be}^+$ .<sup>7</sup> However, the all-order method implemented in Ref. 7

was noted to miss certain terms that contribute to removal energies already at the level of third-order MBPT. In the case of lithium, the missed terms were extremely small, and did not significantly affect the accuracy of the calculations. We have shown,<sup>8,9</sup> however, that when the same methods are applied to cesium the missed terms are much more significant, and must be dealt with in some manner. One way of doing this is the introduction of a “Hermitian conjugate” method.<sup>10</sup> Here we propose a slightly different approach to the problem, building into the formalism a set of triple excitations. The new terms are, however, in many cases similar to terms in the Hermitian formulation.

Both our original all-order scheme employed in Ref. 7 and our new technique are closely related to coupled-cluster methods. Specifically, the former is a linearized version of a coupled-cluster method including single and double excitations. The latter is the extension of this method to include the effect of triple excitations on the single-excitation coefficients. Our new technique is a well-defined calculational scheme that predicts energies and allowed electric dipole ( $E1$ ) matrix elements of cesium accurate to a few tenths of a percent, and hyperfine constants accurate at the 1% level. In addition, we will identify extensions of the method that have the promise of improving the predictions, at the cost of significantly greater computer time, to the one-tenth of a percent level.

The paper is organized as follows. In Sec. II we recapitulate the original all-order method applied to lithium, and introduce a modification to the wave function (involving a triple excitation) that leads to the new all-order equations. In Sec. III a formulation of matrix elements that includes the random-phase approximation (RPA) exactly along with the effect of triple excitations is presented. In Sec. IV computational issues are addressed and numerical results for cesium presented. The concluding section, Sec. V, discusses the further modifications of the method that must be made to reach the next level of accuracy.

## II. ALL-ORDER EQUATIONS

### A. Relativistic, linearized coupled-cluster formalism

The starting point for our relativistic many-body treatment of the cesium atom is the no-virtual-pair Dirac-Coulomb Hamiltonian discussed by Sucher.<sup>11</sup> We write this Hamiltonian as  $H = H_0 + V$ , where (in atomic units  $\hbar = m = e = 4\pi\epsilon_0 = 1$ )

$$H_0 = \sum_{i=1}^N \Lambda_i^+ [c\alpha_i \cdot \mathbf{p}_i + (\beta_i - 1)c^2 + V_{\text{nuc}}(r_i) + U(r_i)] \Lambda_i^+, \quad (1)$$

$$V = \sum_{i>j}^N \Lambda_i^+ \Lambda_j^+ \frac{1}{r_{ij}} \Lambda_j^+ \Lambda_i^+ - \sum_{i=1}^N \Lambda_i^+ U(r_i) \Lambda_i^+. \quad (2)$$

Here we have added an arbitrary potential  $U(r)$  to the model Hamiltonian  $H_0$  and subtracted it again from the perturbation  $V$ ; the potential  $U(r)$  is chosen to approximate the effect of the electron-electron interaction. The nuclear potential  $V_{\text{nuc}}(r)$  includes the effect of finite nuclear size. The  $\Lambda^+$  are projection operators on to the positive-energy states of the Dirac Hamiltonian in the potential  $V_{\text{nuc}} + U(r)$ . As discussed by Sucher, their presence avoids the so-called continuum dissolution problem, and gives the Hamiltonian normalizable, bound-state solutions. Furthermore, the no-virtual-pair Hamiltonian corresponds to a well-defined subset of the full QED atomic perturbation series. Omitted relativistic and field-theoretic effects can be identified and added later in a perturbative manner if desired; these include transverse photon exchange (the Breit interaction), retardation and negative-energy state effects, and radiative corrections. We include Breit-interaction corrections to the hyperfine constants perturbatively, but we omit the remaining corrections, all of which are small for the properties of interest here. The hardest task in neutral cesium is to overcome the many-body problem associated with the dominant Coulomb interaction, which can be approached by means of the no-virtual-pair Hamiltonian. We have still not controlled the many-body problem to sufficient accuracy that the smaller, field-theoretic effects are observable.

In lowest order we choose to work with a  $V^{N-1}$  Dirac-Fock (DF) potential,  $U(r) = V_{\text{DF}}$ , which is the DF potential of the  $N-1$  closed-shell core electrons. A single-particle valence state  $|v\rangle$  then satisfies

$$[c\alpha \cdot \mathbf{p} + (\beta - 1)c^2 + V_{\text{nuc}}(r) + V_{\text{DF}}] |v\rangle = \epsilon_v |v\rangle, \quad (3)$$

$$\langle i | V_{\text{DF}} | j \rangle = \sum_a (g_{iaja} - g_{iaaj}), \quad (4)$$

$$g_{abcd} = \left\langle ab \left| \frac{1}{r_{12}} \right| cd \right\rangle, \quad (5)$$

where the sum over  $a$  in (4) is over all  $N-1$  core states. In second-quantized form,  $H_0$  and  $V$  become for this potential

$$H_0 = \sum_a \epsilon_a + \sum_i \epsilon_i \{a_i^\dagger a_i\}, \quad (6)$$

$$V = -\frac{1}{2} \sum_{a,b} (g_{abab} - g_{abba}) + \frac{1}{2} \sum_{i,j,k,l} g_{ijkl} \{a_i^\dagger a_j^\dagger a_l a_k\}, \quad (7)$$

where braces  $\{ \}$  indicate normal ordering with respect to the core.<sup>1</sup> Here and later we shall adopt the convention that  $a, b, c, \dots$  denote core states,  $n, m, r, \dots$  excited states (including the valence states),  $v$  and  $w$  valence states, and  $i$  and  $j$  general states. The positive-energy projection operators in (1) and (2) restrict all excited states  $n$  and  $m$  to positive-energy states.

The  $V^{N-1}$  DF ground state is an eigenfunction of  $H_0$ , and  $-\epsilon_v$  is the lowest-order approximation to the valence removal energy. The effect of the perturbation  $V$  can be taken into account systematically using the techniques of many-body theory. In earlier work on Cs,<sup>8,9,12</sup> we investigated order-by-order perturbation theory and concluded that, to obtain matrix elements and energies below the 1% level, a scheme that summed certain important subsets of diagrams to all orders is desirable. Dzuba, Flambaum, and Sushkov<sup>13</sup> have recently considered several infinite subsets of diagrams using the time-dependent formulation of many-body theory, and obtained an accuracy below the 1% level. We propose here to use a modification of the coupled-cluster (CC) technique, in a form which contains most of the effects considered by Dzuba, Flambaum, and Sushkov, and several other infinite sequences as well.

Our present technique is an extension of the linearized CC formalism with single and double excitations that we used in our earlier work on Li and Be.<sup>7</sup> The linearized CC formalism is obtained from the complete, open-shell CC formalism (see, e.g., Lindgren and Morrison<sup>1</sup>) by dropping terms which are nonlinear in the cluster operator. This procedure may be outlined as follows. One introduces the exponential ansatz,

$$|\Psi\rangle = [\exp(S)] |\Psi_0\rangle, \quad (8)$$

where  $|\Psi_0\rangle$  is the zeroth-order solution, and  $|\Psi\rangle$  is the exact wave function in intermediate normalization  $\langle \Psi | \Psi_0 \rangle = 1$ . The cluster operator  $S$  can be shown to have a perturbation expansion in terms of purely connected Goldstone diagrams, and to satisfy a generalized Bloch equation,<sup>1,14</sup>

$$[S, H_0]P = (QV\Omega P - \chi P V \Omega P)_{\text{conn}}, \quad (9)$$

where  $P$  is a projection operator on to the state  $|\Psi_0\rangle$ ,  $Q$  is its complement  $Q = 1 - P$ ,  $\Omega = [\exp(S)]$ ,  $\chi = \Omega - 1$ , and "conn" indicates that only connected terms are to be retained on the right-hand side. In the CC method, one solves (9) as a hierarchy of equations for the one-, two-, three-,  $\dots$ , body parts of  $S = S_1 + S_2 + S_3 + \dots$ , where the  $n$ -body part  $S_n$  is defined to excite  $n$  electrons from the state  $|\Psi_0\rangle$ . In the linearized CC used here, we drop the nonlinear terms in the expansion of the exponential  $\Omega = [\exp(S)] = [S + (1/2!)S^2 + (1/3!)S^3 + \dots]$  occurring on the right-hand side of (9). With this assumption, a rather simpler ansatz than (8) would suffice to derive the same equations, but introduction of the full exponential form here is useful for later discussion.

To incorporate single and double excitations to all orders, we truncate  $S$  to  $S = S_1 + S_2$ , where

$$S_1 = \sum_{m,a} \rho_{ma} a_m^\dagger a_a + \sum_m \rho_{mv} a_m^\dagger a_v, \quad (10)$$

$$S_2 = \frac{1}{2} \sum_{m,n,a,b} \rho_{mnab} a_m^\dagger a_n^\dagger a_b a_a + \sum_{m,n,a} \rho_{mnav} a_m^\dagger a_n^\dagger a_v a_a. \quad (11)$$

After substituting these into (9), dropping the nonlinear terms, normally ordering each side with respect to the core, and identifying coefficients of equivalent excitations on each side, one obtains for the valence single excitations and core-valence double excitations

$$(\varepsilon_v + \delta\varepsilon_v - \varepsilon_m) \rho_{mv} = \sum_{b,n,r} g_{mbnr} \tilde{\rho}_{nrvb} - \sum_{b,c,n} g_{bcvn} \tilde{\rho}_{mnbc} + \sum_{b,n} \tilde{g}_{mbvn} \rho_{nb}, \quad (12)$$

$$(\varepsilon_v + \delta\varepsilon_v + \varepsilon_a - \varepsilon_m - \varepsilon_n) \rho_{mnav} = g_{mnav} + \left[ \sum_r g_{mnrv} \rho_{ra} - \sum_c g_{cnav} \rho_{mc} + \sum_{c,r} (g_{ncvr} \tilde{\rho}_{rmca} - g_{cnvr} \rho_{rmca} - g_{ncra} \rho_{rmvc}) \right] + \left[ \begin{array}{c} a \leftrightarrow v \\ m \leftrightarrow n \end{array} \right] \\ + \sum_{c,d} g_{cdva} \rho_{nmcd} + \sum_{r,s} g_{nmrs} \rho_{rsva}, \quad (13)$$

$$\delta\varepsilon_v = \sum_{b,n,r} g_{vbnr} \tilde{\rho}_{nrvb} - \sum_{b,c,n} g_{bcvn} \tilde{\rho}_{vnbc} + \sum_{b,n} \tilde{g}_{vbvn} \rho_{nb}, \quad (14)$$

where the tilde notation denotes the inclusion of exchange,  $\tilde{\rho}_{abcd} = \rho_{abcd} - \rho_{bacd}$ , and  $-\delta\varepsilon_v$  is the correlation correction to the valence removal energy. A similar set of equations holds for core excitations, but with no  $\delta\varepsilon_v$  in the energy factor on the left, and with  $v$  replaced by  $a$  for core single excitations, and by  $b$  for core-core double excitations. The core equations are independent of the valence state  $v$ , and give the solution for the closed-shell  $N-1$  particle core, while the valence equations give the effect of adding the  $N$ th electron. We solve the core equations first, store the coefficients, and then solve the valence equations for each valence state of interest.

By inspection one can show that while terms missed in this formalism occur first in fourth order for the total core energy, they occur already in third order for the more interesting valence removal energy. To pick up the set of missed third-order diagrams in the standard CC approach would require the introduction of triple excitations, as shown in Fig. 1. These missed terms are large for Cs: they contribute about  $-1.8\%$  to the  $6s$  valence removal energy,<sup>8,9</sup> and about  $-4\%$  to the  $6s$  hyperfine constant. They are numerically the next most important

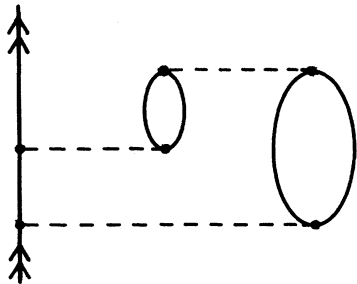


FIG. 1. Example of a third-order contribution to the valence removal energy arising from triple excitations in the standard CC approach. Removal of the uppermost Coulomb interaction leaves the underlying term from  $S_3$ .

modification to the linearized singles and doubles approach outlined above, and must be included to obtain reasonable agreement for Cs.

### B. Inclusion of a subset of triple excitations

As shown in Sec. IV, the basis set we use is sufficiently large that it is not possible to store triple-excitation coefficients  $\rho_{nmrabc}$ . We thus avoid the explicit introduction of such coefficients, and instead derive terms which give their contribution to the single and double coefficients. Our scheme is as follows. The leading contribution to the  $S_3$  operator arises from the second-order terms in Fig. 2, which are the triple-excitation part of  $VS_2$ . Schematically,  $S_3$  in this approximation is given by

$$D_3 S_3 = \{VS_2\}_{3,\text{conn}}. \quad (15)$$

This shorthand notation indicates that  $VS_2$  is normally ordered, retaining only connected, triple excitations; each excitation is identified with the corresponding one on the left-hand side, and  $D_3$  signifies a triple-excitation energy factor, given by  $(\varepsilon_a + \varepsilon_b + \varepsilon_c - \varepsilon_n - \varepsilon_m - \varepsilon_r)$  for an excitation  $abc \rightarrow nmr$ , for example. We can now determine the effect of  $S_3$  in this approximation on the single- and double-excitation coefficients,

$$D_1 S_1 = \dots + \left\{ V \frac{1}{D_3} \{VS_2\}_{3,\text{conn}} \right\}_{1,\text{conn}}, \quad (16)$$

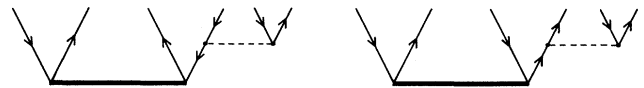


FIG. 2. Leading contribution to  $S_3$  (for a core-core-core excitation). The solid line indicates a double-excitation coefficient from  $S_2$ .

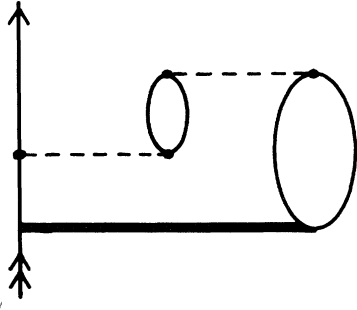


FIG. 3. A sample term from  $\{V(1/D_3)\{VS_2\}_{3,conn}\}_{1,conn}$ . It is topologically similar to Fig. 1, except that the lowest Coulomb interaction is replaced by an all-order double-excitation coefficient.

$$D_2 S_2 = \cdots + \left\{ V \frac{1}{D_3} \{VS_2\}_{3,conn} \right\}_{2,conn}. \quad (17)$$

We have implemented only the modification to the single-excitation equation in the present work, and shall confine our subsequent discussion to this term.

Let us consider the sample term from Eq. (16) shown in Fig. 3, and given explicitly by

$$\begin{aligned} & (\varepsilon_v + \delta\varepsilon_v - \varepsilon_m) \rho_{mv} \\ &= \cdots + \sum_{b,c,n,r,s} \frac{\tilde{g}_{bcrs} \tilde{g}_{mrnb} \tilde{\rho}_{nsvc}}{\varepsilon_v + \varepsilon_b + \varepsilon_c - \varepsilon_r - \varepsilon_m - \varepsilon_s} + \cdots \end{aligned} \quad (18)$$

This term is topologically similar to the missed third-order energy diagram in Fig. 1; in fact, the effect of (16) is to reproduce the entire set of missed third-order terms, with the lower Coulomb matrix element replaced by a double-excitation coefficient. Before coding these terms, however, we make one further manipulation. To

$$\begin{aligned} (\varepsilon_v + \delta\varepsilon_v - \varepsilon_m) \rho_{mv} &= \cdots + \sum_{b,c,n,r,s} (\tilde{\rho}_{rsbc})^* \tilde{g}_{mrnb} \tilde{\rho}_{nsvc} - \sum_{b,c,d,n,s} (\tilde{\rho}_{sncd})^* \tilde{g}_{sbvc} \tilde{\rho}_{mnb} + \sum_{b,c,d,s,t} (\rho_{stbc})^* \tilde{g}_{mdbc} \tilde{\rho}_{stcd} \\ &- \sum_{b,d,n,s,t} (\rho_{stbd})^* \tilde{g}_{tsnv} \tilde{\rho}_{mnb} + \sum_{b,c,n,s,t} (\tilde{\rho}_{ntbc})^* \tilde{g}_{mnvs} \rho_{stbc} - \sum_{b,c,d,s,t} (\tilde{\rho}_{stbd})^* \tilde{g}_{mcvb} \rho_{stcd} \\ &+ \sum_{b,c,n,s,t} (\tilde{\rho}_{ntcb})^* \tilde{g}_{ntsb} \tilde{\rho}_{msvc} - \sum_{b,c,d,s,t} (\tilde{\rho}_{stbd})^* \tilde{g}_{ctbd} \tilde{\rho}_{msvc}. \end{aligned} \quad (21)$$

These terms are to be added to the right-hand side of the valence single-excitation equation (12). The modification to the core single-excitation equation is obtained by replacing  $v$  by  $a$  in the right-hand side of the above. The formula for  $\delta\varepsilon_v$  is modified by adding terms obtained by

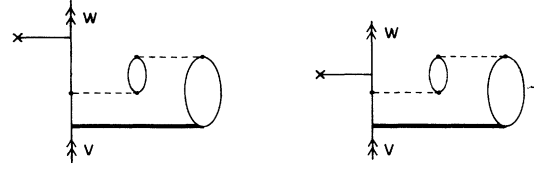


FIG. 4. Two contributions to the matrix element of a one-body operator associated with the term in Fig. 3.

motivate it, we consider the two contributions of (18) to the matrix element of a one-body operator shown in Fig. 4. Upon adding these two terms, the triple-excitation energy denominator simplifies to a double excitation,

$$\begin{aligned} & \sum_{b,c,m,n,r,s} \frac{z_{wm} \tilde{g}_{bcrs} \tilde{g}_{mrnb} \tilde{\rho}_{nsvc}}{(\varepsilon_v + \varepsilon_b + \varepsilon_c - \varepsilon_r - \varepsilon_m - \varepsilon_s)} \\ & \times \left[ \frac{1}{(\varepsilon_v - \varepsilon_m)} + \frac{1}{(\varepsilon_b + \varepsilon_c - \varepsilon_r - \varepsilon_s)} \right] \\ &= \sum_{b,c,m,n,r,s} \frac{z_{wm} \tilde{g}_{bcrs} \tilde{g}_{mrnb} \tilde{\rho}_{nsvc}}{(\varepsilon_v - \varepsilon_m)(\varepsilon_b + \varepsilon_c - \varepsilon_r - \varepsilon_s)}, \end{aligned} \quad (19)$$

and the expression now contains the factor  $\tilde{g}_{bcrs}/(\varepsilon_b + \varepsilon_c - \varepsilon_r - \varepsilon_s)$  which is just the lowest-order approximation to  $(\tilde{\rho}_{rsbc})^*$ . It can be shown similarly that energy denominator simplifications occur when the new terms in  $S_1$  contribute to the right-hand side of the double-excitation equation, and that furthermore the combination  $\tilde{g}_{bcrs}/(\varepsilon_b + \varepsilon_c - \varepsilon_r - \varepsilon_s)$  can be generalized to the all-order doubles coefficient  $(\tilde{\rho}_{rsbc})^*$ . We thus modify the term in Eq. (18) to

$$(\varepsilon_v + \delta\varepsilon_v - \varepsilon_m) \rho_{mv} = \cdots + (\tilde{\rho}_{rsbc})^* \tilde{g}_{mrnb} \tilde{\rho}_{nsvc} + \cdots \quad (20)$$

We obtain the complete set of terms from (16) in this way,

replacing  $m$  by  $v$  in the above. The complete set of all-order equations is shown graphically in Figs. 5 and 6.

The terms derived here are similar to terms occurring in the Hermitian formulation of the CC method discussed by Lindgren and others,<sup>10</sup> except that here we have not

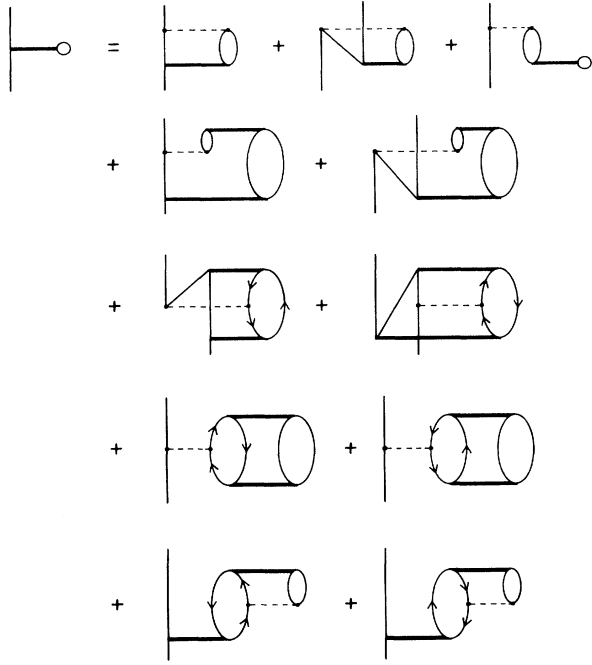


FIG. 5. All-order equations for single excitations used in the present work. The solid line indicates a double-excitation coefficient, while the solid line terminated by a circle indicates a single-excitation coefficient.

changed the normalization as discussed by these authors, but retained intermediate normalization. The new terms are also similar to terms discussed by Bartlett.<sup>15</sup>

### III. MATRIX-ELEMENT FORMALISM

We next discuss our approach for using the single- and double-excitation coefficients derived above to calculate

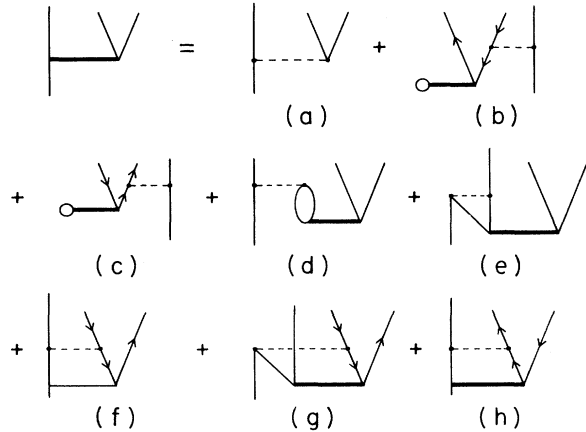


FIG. 6. All-order equations for double excitations used in the present work. The solid line indicates a double-excitation coefficient, while the solid line terminated by a circle indicates a single-excitation coefficient.

the matrix element of a sum of one-body operators  $Z = \sum_{i=1}^N z_i$ ,

$$M_{wv} = \frac{\langle \Psi_w | Z | \Psi_v \rangle}{\sqrt{\langle \Psi_w | \Psi_w \rangle \langle \Psi_v | \Psi_v \rangle}}. \quad (22)$$

Before substituting our approximation to the exact wave functions  $|\Psi_v\rangle$  and  $|\Psi_w\rangle$  into this expression, we note that the effect of the denominator is to cancel disconnected terms from the numerator. While this cancellation is well known to be complete for closed-shell states, we showed previously<sup>7</sup> that for one-valence-electron states there is a residual normalization factor,

$$M_{wv} = M_{\text{core}} + \frac{M_{\text{val}}}{\sqrt{(1+N_w)(1+N_v)}}, \quad (23)$$

$$M_{\text{core}} = \delta_{wv} \langle 0_C | \Omega_w^\dagger Z \Omega_v | 0_C \rangle_{\text{conn}}, \quad (24)$$

$$M_{\text{val}} = \langle 0_C | \overline{a_w (\Omega_w^\dagger Z \Omega_v) a_v^\dagger} | 0_C \rangle_{\text{conn}}, \quad (25)$$

$$N_v = \langle 0_C | \overline{a_v (\Omega_v^\dagger \Omega_v) a_v^\dagger} | 0_C \rangle_{\text{conn}}, \quad (26)$$

where  $|0_C\rangle$  is the core determinant, and  $|\Psi_v\rangle = \Omega_v a_v^\dagger |0_C\rangle$ . The bar notation in (25) and (26) signifies that  $a_w$  (or  $a_v$ ) and  $a_v^\dagger$  contract into the intervening parentheses. The Goldstone diagrams for  $M_{\text{val}}$  and  $N_v$  thus involve one ingoing and one outgoing valence line, while those for  $M_{\text{core}}$  are closed.  $M_{\text{core}}$  vanishes for nonscalar operators  $Z$ , with which we are concerned here, and we shall not discuss it further.

Substitution of the approximate wave function into (23) rather than (22) explicitly removes spurious disconnected terms from the expression. We showed previously<sup>7</sup> that this substitution gives in the linearized CC approximation an expression involving 21 terms for  $M_{\text{val}}$  and five terms for  $N_v$ . The explicit expressions are given in Ref. 7; three sample diagrams are shown in Fig. 7. However, as was noted in Ref. 7, this formalism does not include the RPA exactly, but misses certain RPA terms from fourth-order onwards. We have found special sensitivity of excited-state dipole-matrix elements, e.g.,  $\langle 9p_{1/2} | D | 6s \rangle$ , to the omitted RPA terms, and have therefore modified the formalism to incorporate the RPA exactly.

Our first step is to calculate the RPA vertex (with exchange) for a one-body operator, given by

$$z_{ij}^{\text{RPA}}(\omega) = z_{ij} + \sum_{am} \left[ \frac{\tilde{g}_{imja} z_{am}^{\text{RPA}}(\omega)}{\epsilon_a - \omega - \epsilon_m} + \frac{\tilde{g}_{iajm} z_{ma}^{\text{RPA}}(\omega)}{\epsilon_a + \omega - \epsilon_m} \right], \quad (27)$$

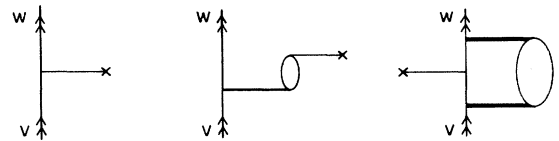


FIG. 7. Three sample terms from the expression derived in Ref. 7 for the matrix element of a one-body operator. The one-body operator is denoted by a solid line terminated by a cross.

and shown graphically in Fig. 8. This vertex is to be evaluated at a frequency  $\omega$  which we set equal to the experimental frequency for the transition,  $\omega = (E_w - E_v)^{\text{expt}}$ , or equal to zero for diagonal-matrix elements; we have found a negligible sensitivity to small variations of  $\omega$  about these values. To construct  $z^{\text{RPA}}(\omega)$ , we first solve (27) iteratively for the core-excited matrix elements,  $z_{ma}^{\text{RPA}}(\omega)$  and  $z_{am}^{\text{RPA}}(\omega)$ ; these are stored and used later to calculate a general matrix element  $z_{ij}^{\text{RPA}}(\omega)$ .

The bare vertex is now replaced everywhere by the RPA vertex in the expressions derived in Ref. 7 for the linearized CC. Clearly, however, this leads to a double-counting of effects, one example of which is shown in Fig. 9. Furthermore, simply deleting the diagrams containing doubly counted effects in general also removes effects that are singly counted and numerically important. Our strategy is to remove the diagrams containing doubly counted effects, and add back the singly counted effects by explicit construction; this is explained in Figs. 9 and 10.

Our final set of matrix-element terms is shown graphically in Fig. 11. We present the matrix element as a sum of six terms,  $M_{wv} = M^{(1)} + M^{\text{RPA}} + M^{\text{BO}} + M^{\text{SR}} + M^{\text{other}} + M^{\text{norm}}$ , where  $M^{(1)}$  is the lowest-order matrix element,  $M^{\text{RPA}}$  the RPA correction,  $M^{\text{BO}}$  is a correction associated with Brueckner or natural orbitals,  $M^{\text{SR}}$  is a *structural radiation* correction, and  $M^{\text{norm}}$  accounts for the normalization denominator in (23). Some remaining terms are given by  $M^{\text{other}}$ . The explicit analytical expressions are

$$M^{(1)} = z_{wv}, \quad (28)$$

$$M^{\text{RPA}} = z_{wv}^{\text{RPA}} - z_{wv}, \quad (29)$$

$$M^{\text{BO}} = M^{(b)} + M^{(c)} + \dots + M^{(k)},$$

$$M^{(b)} = - \sum_a z_{av}^{\text{RPA}} \rho_{wa} + \text{c.c.},$$

$$M^{(c)} = \sum_m z_{wm}^{\text{RPA}} \rho_{mv} + \text{c.c.},$$

$$M^{(d)} = - \sum_{a,b,m,n} \rho_{nmwa}^* z_{bv}^{\text{RPA}} \tilde{\rho}_{mnab} + \text{c.c.},$$

$$M^{(e)} = - \sum_{a,b,m,n} \rho_{mnbv}^* z_{mv}^{\text{RPA}} \tilde{\rho}_{nwab} + \text{c.c.},$$

$$M^{(f)} = - \sum_{a,b,m} \rho_{ma}^* z_{bv}^{\text{RPA}} \tilde{\rho}_{wmba} + \text{c.c.}, \quad (30)$$

$$M^{(g)} = \sum_{a,m,n} \tilde{\rho}_{mnwa}^* z_{mv}^{\text{RPA}} \rho_{na} + \text{c.c.},$$

$$M^{(h)} = \sum_{m,n} \rho_{nw}^* z_{nm}^{\text{RPA}} \rho_{mv},$$

$$M^{(i)} = - \sum_{a,m} \rho_{mw}^* z_{av}^{\text{RPA}} \rho_{ma} + \text{c.c.},$$

$$M^{(j)} = - \sum_{a,m} \rho_{ma}^* z_{mv}^{\text{RPA}} \rho_{wa} + \text{c.c.},$$

$$M^{(k)} = \sum_{a,b} \rho_{vb}^* z_{ab}^{\text{RPA}} \rho_{wa};$$

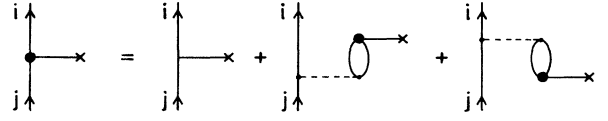


FIG. 8. Graphical definition of the RPA vertex for a one-body operator.

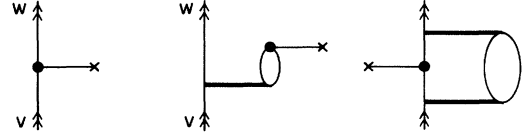


FIG. 9. The three diagrams in Fig. 7 generalized the replacement of the bare one-body operator by the RPA vertex given in Fig. 8. Diagram (b) contains implicitly RPA terms already present in diagram (a), and therefore represents a double counting.

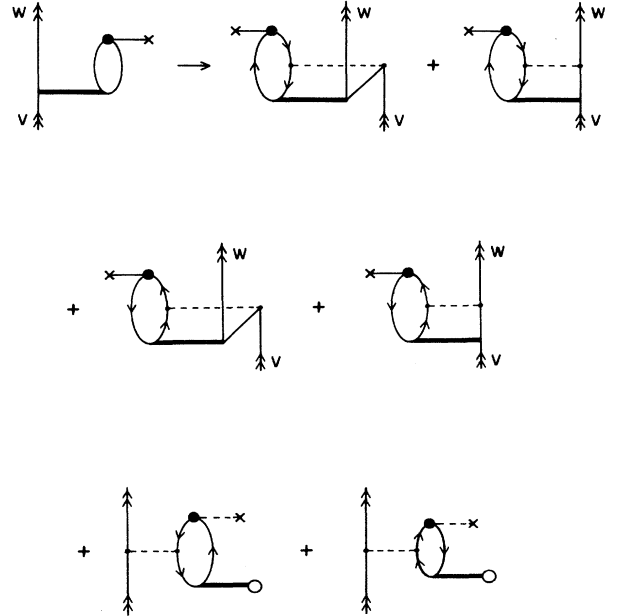


FIG. 10. Substitution made to remove doubly counted RPA effects. The substitution is obtained by replacing the double excitation coefficient by all terms on the right-hand side of the double-excitation equation, Fig. 7, and removing those terms which are included elsewhere in the matrix-element expression.

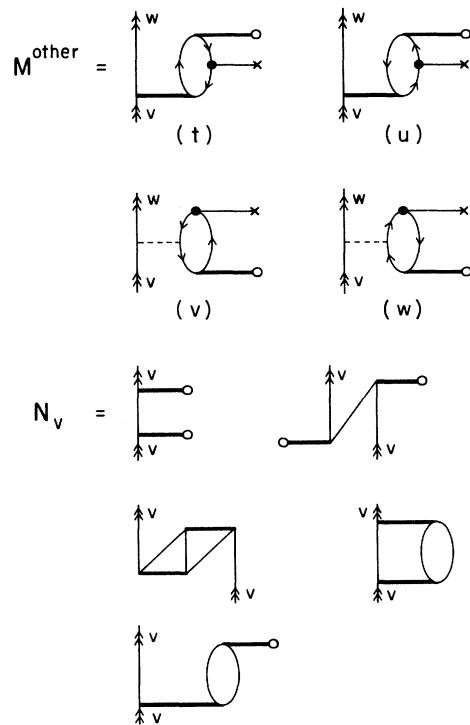
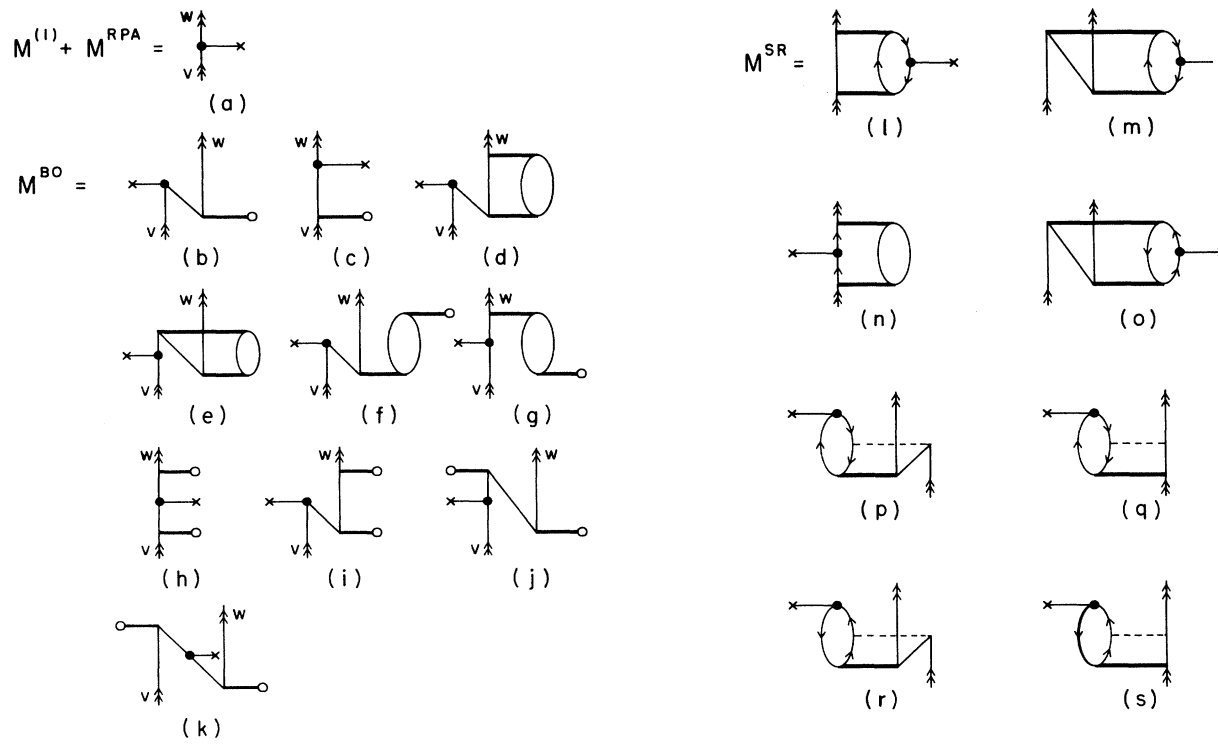


FIG. 11. Complete expression for the matrix element used in present work.

$$\begin{aligned}
M^{\text{SR}} &= M^{(1)} + M^{(m)} + \dots + M^{(s)}, \\
M^{(l)} &= - \sum_{a,b,m,n} \rho_{nmwb}^* z_{ab}^{\text{RPA}} \tilde{\rho}_{nmva}, \\
M^{(m)} &= \sum_{a,b,c,m} \tilde{\rho}_{vmbc}^* z_{ac}^{\text{RPA}} \tilde{\rho}_{wmba}, \\
M^{(n)} &= \sum_{a,m,n,r} \tilde{\rho}_{rnwa}^* z_{rm}^{\text{RPA}} \tilde{\rho}_{mnva}, \\
M^{(o)} &= - \sum_{a,b,m,n} \rho_{vmba}^* z_{mn}^{\text{RPA}} \tilde{\rho}_{nwab}, \\
M^{(p)} &= \sum_{a,b,c,m} z_{bm}^{\text{RPA}} g_{cab} \tilde{\rho}_{mwca} + \text{c.c.}, \\
M^{(q)} &= - \sum_{a,b,m,n} z_{am}^{\text{RPA}} \tilde{g}_{bwan} \tilde{\rho}_{mnbv} + \text{c.c.}, \\
M^{(r)} &= - \sum_{a,b,m,n} z_{am}^{\text{RPA}} \tilde{g}_{mbnv} \tilde{\rho}_{nwab} + \text{c.c.}, \\
M^{(s)} &= \sum_{a,m,n,r} z_{am}^{\text{RPA}} g_{mwnr} \tilde{\rho}_{nrav} + \text{c.c.}; \\
M^{\text{other}} &= M^{(t)} + M^{(u)} + \dots + M^{(w)}, \\
M^{(t)} &= - \sum_{a,b,m} \rho_{mb}^* z_{ab}^{\text{RPA}} \tilde{\rho}_{wmva} + \text{c.c.}, \\
M^{(u)} &= \sum_{a,m,n} \rho_{ma}^* z_{mn}^{\text{RPA}} \tilde{\rho}_{wnva} + \text{c.c.}, \\
M^{(v)} &= - \sum_{a,b,m} z_{am}^{\text{RPA}} \tilde{g}_{wbva} \rho_{mb} + \text{c.c.}, \\
M^{(w)} &= \sum_{a,m,n} z_{am}^{\text{RPA}} \tilde{g}_{wmvm} \rho_{na} + \text{c.c.}; \\
M^{\text{norm}} &= [M^{(1)} + M^{\text{RPA}} + M^{\text{BO}} + M^{\text{SR}} + M^{\text{other}}] \\
&\quad \times [(1+N_w)^{-1/2} (1+N_v)^{-1/2} - 1], \\
N_v &= \sum_m \rho_{mv}^* \rho_{mv} - \sum_a \rho_{va}^* \rho_{va} \\
&\quad + \sum_{a,b,m} \rho_{vmab}^* \tilde{\rho}_{mvab} + \sum_{a,m,n} \rho_{mnva}^* \tilde{\rho}_{mnva} \\
&\quad + \sum_{m,a} (\tilde{\rho}_{vmva} \rho_{ma}^* + \tilde{\rho}_{vmva}^* \rho_{ma}).
\end{aligned} \tag{31}$$

Here "c.c." denotes complex conjugation and interchange of  $v$  and  $w$ .

We have not added back all possible singly counted effects here; some small terms, such as the one shown in Fig. 12, have been neglected.

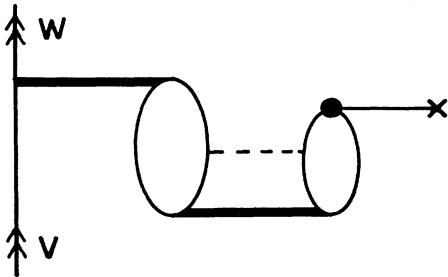


FIG. 12. A diagram neglected in the present work which contains only single or double excitations.

#### IV. NUMERICAL PROCEDURE AND RESULTS

We solve the equations presented in Secs. II and III by means of a relativistic finite basis set constructed from piecewise polynomials or *B splines*.<sup>16</sup> In this approach, the infinite sum over excited states  $n, m, \dots$ , etc. (strictly, a sum over an infinite set of bound states plus an integral over positive-energy continuum states) is replaced by a finite sum over a set of pseudostates. Because the separation of positive- and negative-energy states in the pseudospectrum is clean, the projection operators in the no-virtual-pair Hamiltonian [(1) and (2)] can be implemented directly by summing over only the positive-energy half of the pseudospectrum. For  $s$  and  $p$  states, we use a basis set consisting of 25 positive-energy states; for higher angular momenta, we use 20 positive-energy states. We include all angular momenta up to  $l=7$  (i.e.,  $k$  states); since in a relativistic formalism there are two  $j$  values for each nonzero orbital angular momentum (e.g.,  $p_{1/2}$  and  $p_{3/2}$ ), we thus include 15 different angular momentum values in all. This basis set is sufficiently complete as to reduce the basis-set truncation error in the second-order valence removal energy to below 1.0% of the correlation energy.

The number of channels that we include for the single and double excitations is determined by the following considerations. For the parity nonconservation problem, and for  $s$ -state hyperfine constants, the physically important region is near the origin, and the contribution of the deep core states is quite important. For example, there are many-body effects associated with excitation of the  $1s$  and  $2s$  states that contribute about 0.8% each to the  $6s$  hyperfine constant. We have thus excited *all* core states, and include all possible single- and double-excitation channels consistent with our basis set. The total number of coefficients is kept to a manageable size by working with *radial* excitation coefficients,<sup>1</sup> and by performing the sum over magnetic quantum numbers analytically. We shall define a double-excitation "channel" to be specified by the quantum numbers  $ab \rightarrow \kappa_n \kappa_m(L)$ , where  $a$  and  $b$  are core states,  $\kappa_n$  is the angular-quantum number for excited states  $n$ , and  $L$  is the multipolarity of the radial doubles coefficient (similar to the multipolarity of the radial Slater integral which occurs in Coulomb matrix elements). For each channel, there are  $n_n n_m$  double-excitation coefficients, where  $n_n$  is the number of states in the basis set for angular momentum  $\kappa_n$ . For the calculations presented in this section, we include in all about 16 000 channels, requiring about 10 megawords of computer storage; the calculation was performed in core memory on a Cray-2 supercomputer. It is easy to appreciate, however, that for a basis set of this size it would be impossible to store triple-excitation coefficients, unless gross restrictions were made on the number of channels included.

It should be emphasized that the number of channels required is greatly increased by the use of a relativistic formalism: in a fully nonrelativistic approach, there is no need to distinguish between the two different  $j$  values for a given  $l$ .

The computationally expensive step in the calculation



TABLE I. Valence removal energies (a.u.).

State	$\epsilon_v^{\text{DHF}}$	$\delta\epsilon_v$	Sum	Experiment <sup>a</sup>	$\Delta(\%)$
6s	0.127 37	0.015 21	0.142 57	0.143 10	-0.37
7s	0.055 19	0.003 26	0.058 45	0.058 65	-0.33
6p <sub>1/2</sub>	0.085 62	0.006 36	0.091 98	0.092 17	-0.21
7p <sub>1/2</sub>	0.042 02	0.001 83	0.043 85	0.043 93	-0.17
8p <sub>1/2</sub>	0.025 12	0.000 80	0.025 92	0.025 96	-0.14
6p <sub>3/2</sub>	0.083 79	0.005 72	0.089 51	0.089 64	-0.15
7p <sub>3/2</sub>	0.041 37	0.001 66	0.043 03	0.043 10	-0.16
8p <sub>3/2</sub>	0.024 81	0.000 74	0.025 55	0.025 58	-0.13

<sup>a</sup>C. E. Moore, *Atomic Energy Levels*, Natl. Bur. Stand. Ref. Data Ser., Natl. Bur. Stand. (U.S.) Circ. No. 35 (U.S. GPO, Washington, D.C., 1971), Vol. I.

is the convergence of the all-order equations. The most expensive term to evaluate is the particle-particle ladder [Fig. 6(h)], which involves summation over four excited states, and which is individually an important contribution (about -3% for the 6s ionization energy). However, as is discussed in Refs. 13 and 9, there is a partial cancellation between the particle-particle ( $p$ - $p$ ) and the particle-hole ( $p$ - $h$ ) ladders [Figs. 6(h) and 6(f)]. We make use of this cancellation to accelerate the convergence of the solution. As a first step, we solve the coupled single- and double-excitation equations omitting (i) the  $p$ - $p$  and  $p$ - $h$  ladders, and (ii) the triple-excitation terms in the singles equation. Then, we perform three full iterations including all terms. For the  $p$ - $p$  and  $p$ - $h$  ladder diagrams only, we restrict the maximum orbital angular momentum of included states to four for core-core double excitations, and to five for core-valence double excitations; this approximation introduces negligible error.

We present results for valence removal energies in Table I, for hyperfine constants in Table II, and for electric dipole transition amplitudes in Table III. Note that for magnetic dipole hyperfine constants we include the

effect of finite nuclear magnetization distribution by assuming a uniformly magnetized sphere of radius 5.7 fm. The effect is significant: for 6s, the hyperfine constant is reduced by 0.6% relative to that arising from a point magnetic dipole.

## V. DISCUSSION AND CONCLUSIONS

Because of the large size of our basis set, the discrepancies with experiment noted in Tables I–III should be explained almost entirely by omitted correlation effects. For valence removal energies, the formalism is complete through third order, and we classify the omitted fourth-order effects into two broad categories: (i) nonlinear terms, which can be accounted for by including the nonlinear terms in the CC *ansatz* (8), and (ii) triple excitations.

We can make a crude estimate of some of these fourth-order terms as follows. The two dominant effects in category (i) arise from including the terms  $S_1S_2$  and  $\frac{1}{2}S_2^2$  in the expansion of  $[\exp(S)]$ ; the former contributes directly to the single-excitation equation, and hence to

TABLE II. Magnetic dipole hyperfine constants (MHz) for  $^{133}\text{Cs}$ ,  $I = \frac{7}{2}$ ,  $g_I = 0.737\,720\,8$  Conversion factor: 1 a.u. =  $6.579\,684 \times 10^9$  MHz.

State	$M^{(1)}$	$M^{\text{RPA}}$	$M^{\text{BO}}$	$M^{\text{SR}}$	$M^{\text{other}}$	$M^{\text{norm}}$	$M^{\text{Breit}}$	Sum	Expt. <sup>a</sup>	$\Delta(\%)$
6s	1426.81	292.83	596.85	4.66	26.23	-56.39	-0.00	2291.00	2298.16	-0.31
7s	392.05	79.64	76.58	0.76	6.54	-11.49	-0.05	544.04	545.90(9) <sup>b</sup>	-0.34
6p <sub>1/2</sub>	161.09	39.93	84.67	9.67	3.06	-4.49	-1.25	292.67	291.90(13)	0.27
7p <sub>1/2</sub>	57.68	13.68	20.54	3.15	1.01	-1.46	-0.39	94.21	94.35(4)	-0.15
8p <sub>1/2</sub>	27.11	6.32	8.34	1.39	0.46	-0.66	-0.17	42.79	42.97(10)	-0.43
6p <sub>3/2</sub>	23.944	18.853	16.226	-9.321	0.890	-0.675	-0.131	49.785	50.275(3) <sup>c</sup>	-0.97
7p <sub>3/2</sub>	8.650	6.700	3.948	-3.083	0.303	-0.220	-0.043	16.255	16.605(6)	-2.11
8p <sub>3/2</sub>	4.087	3.146	1.610	-1.415	0.140	-0.100	-0.020	7.447	7.58(1)	-1.75

<sup>a</sup>E. Arimondo, M. Inguscio, and P. Violino, *Rev. Mod. Phys.* **49**, 31 (1977).

<sup>b</sup>S. L. Gilbert, R. N. Watts, and C. E. Wieman, *Phys. Rev. A* **27**, 581 (1983).

<sup>c</sup>C. Tanner and C. E. Wieman, *Phys. Rev. A* **38**, 1616 (1988).

TABLE III. Reduced  $E1$  transition-matrix elements for length ( $L$ ) and velocity ( $V$ ) forms of dipole operator (a.u.).

Transition	$M^{(1)}$	$M^{RPA}$	$M^{BO}$	$M^{SR}$	$M^{other}$	$M^{norm}$	Sum	Expt. <sup>a</sup>	$\Delta \pm \Delta^{expt}$ (%)
$6s-6p_{1/2}$	$L$	0.303	0.404	-0.040	-0.005	0.090	-4.525	-4.52(1)	0.11±0.22
	$V$	-4.129	-0.505	-0.051	-0.002	0.090	-4.492		
$6s-7p_{1/2}$	$L$	0.372	0.028	0.017	0.002	-0.006	0.279	0.284(2)	-1.74±0.70
	$V$	0.263	-0.077	0.010	0.001	-0.006	0.275		
$6s-8p_{1/2}$	$L$	0.1326	-0.0838	0.0194	0.0010	-0.0016	0.0787		
	$V$	0.0835	-0.0515	0.0407	0.0004	-0.0015	0.0772		
$6s-6p_{3/2}$	$L$	-7.426	0.413	0.582	-0.053	0.121	-6.370	-6.36(1)	0.15±0.16
	$V$	-5.761	0.119	-0.722	-0.078	-0.007	0.121	-6.328	
$6s-7p_{3/2}$	$L$	-0.695	0.187	-0.052	-0.024	0.011	-0.575	-0.583(10)	-1.38±1.72
	$V$	-0.508	0.098	-0.151	-0.018	-0.002	0.011	-0.571	
$6s-8p_{3/2}$	$L$	-0.283	0.118	-0.036	-0.015	0.004	-0.214		
	$V$	-0.196	0.067	-0.076	-0.009	-0.001	-0.212		
$7s-6p_{1/2}$	$L$	-4.413	-0.037	0.140	0.006	0.077	-4.228		
	$V$	-3.854	-0.189	-0.247	-0.039	0.000	-4.251		
$7s-7p_{1/2}$	$L$	-11.009	0.088	0.410	-0.008	0.189	-10.332		
	$V$	-9.653	-0.108	-0.650	-0.041	0.000	-10.264		
$7s-8p_{1/2}$	$L$	-0.921	0.052	-0.059	-0.005	0.017	-0.917		
	$V$	-0.788	-0.007	-0.125	-0.012	0.000	-0.916		
$7s-6p_{3/2}$	$L$	-6.671	-0.042	0.144	0.008	0.112	-6.451		
	$V$	-5.899	-0.298	-0.351	-0.064	-0.004	-6.503		
$7s-7p_{3/2}$	$L$	15.345	-0.117	-0.634	0.010	-0.248	14.357		
	$V$	13.352	0.174	0.917	0.063	-0.247	14.265		
$7s-8p_{3/2}$	$L$	1.605	-0.071	0.109	0.007	-0.028	1.624		
	$V$	1.382	0.022	0.224	0.019	-0.028	1.620		

<sup>a</sup>L. Shabanova, Yu. Monakov, and A. Khlyustalov, Opt. Spektrosk. **47**, 3 (1979) [Opt. Spectrosc. (USSR) **47**, 1 (1979)].

the valence removal energy, while the latter contributes only indirectly through a modification to the double-excitation coefficients. Two sample fourth-order diagrams are given in Fig. 13. We can estimate the effect of  $S_1 S_2$  by noting that it contributes certain terms to the chaining of the self-energy, in which the connecting line is a core state.<sup>8</sup> This core contribution to chaining may be calculated along the lines discussed in Ref. 8, and we find that it contributes  $-0.2\%$  to the valence removal energy for  $6s$  (about  $-2\%$  of correlation).

Turning to the omitted fourth-order triples, we give several examples in Fig. 14. We have discussed these diagrams previously,<sup>9</sup> and recently Salomonson and Ynnerman<sup>17</sup> have evaluated similar diagrams for Na, finding a contribution on the order of  $+5\%$  of correlation. Assuming a similar situation holds in Cs, we would obtain a contribution on the order of  $0.5\%$  to  $1.0\%$  to the  $6s$  valence removal energy. It is possible that the accuracy obtained in the present work for the removal energies arises from a partial cancellation of omitted nonlinear terms and omitted triple-excitation terms.

The matrix-element calculation is complete through third order. In fourth order, a few small terms are missing that could in principle be included at the single- and double-excitation level, e.g., Fig. 12. However, we expect the most serious fourth-order omission to arise from triple excitations, specifically from those terms in which the internal lines of RPA diagrams are modified by insertion of a self-energy, an example of which is shown in Fig. 15. Indeed, certain effects of this type are associated with single and double excitations, and have been evaluated from Figs. 11(t)–11(w), giving contributions on the order of  $1\%$  for the  $6s$  hyperfine constant.

A second important type of error in the matrix element arises in fifth order and is closely connected with the error in the valence removal energies. The Brueckner orbital contribution  $M^{BO}$  is numerically very important, and is dominated by the terms involving valence single excitations. Thus, fourth-order errors in the valence removal energy imply corresponding fifth-order errors in  $M^{BO}$ . We can estimate the probable size of these omitted terms by assuming a scaling argument, namely, that the contribution  $M^{BO}$  scales in approximately the same way as the correlation correction  $\delta\varepsilon_v$  to the valence removal energy as more effects are added. We have observed such an approximate scaling behavior in lower orders. To implement the scaling, we reevaluate the matrix element with all valence single-excitation coefficients  $\rho_{mv}$  replaced by  $\lambda\rho_{mv}$ , where  $\lambda = (\delta\varepsilon_v)^{\text{expt}}/(\delta\varepsilon_v)^{\text{calc}}$  is the ratio of experimental to calculated correlation energies. This pro-

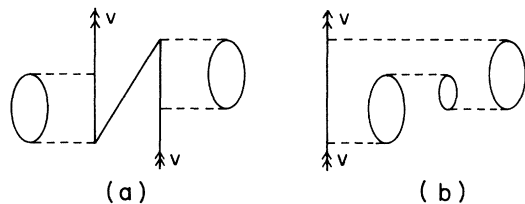


FIG. 13. Sample fourth-order contributions to valence removal energy associated with nonlinear terms: (a)  $S_1 S_2$ , (b)  $\frac{1}{2} S_2^2$ .

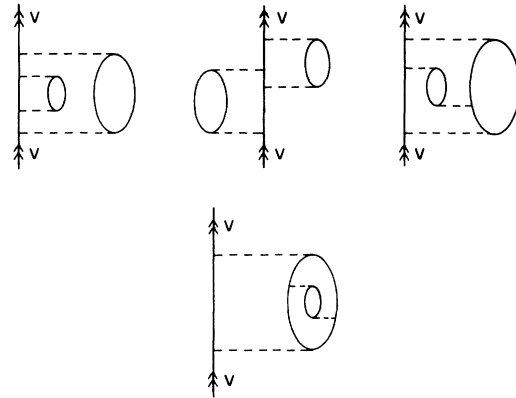


FIG. 14. Sample fourth-order terms containing triple excitations.

cedure is similar to the fitting of energies discussed by Dzuba, Flambaum, and Sushkov.<sup>13</sup> The results are presented in Table IV. We conclude that there are omitted terms of this type entering at the  $1\%$  level for hyperfine constants, and at the few tenths of a percent level for dipole-matrix elements.

Taking all the tests discussed above into account, as well as the explicit comparison with experiment given in Tables I–III, we conclude that the method presented in this paper gives valence removal energies accurate to about  $0.5\%$  or better ( $5\%$  of correlation), hyperfine constants accurate to about  $1\%$ , and electric dipole transition-matrix elements accurate to  $0.5\%$  or better (the level of experimental error).

We now briefly compare the calculation performed here with the all-order approach of Dzuba, Flaumbaum, and Sushkov.<sup>13</sup> A direct comparison of the two calculations is difficult, because Dzuba, Flaumbaum, and Sushkov use the time-dependent formulation, rather than the time-independent formulation of many-body theory which is used here. We have given some comparison of these two approaches in Ref. 9; there we discussed how the present approach contains the most important effects considered by Dzuba, Flaumbaum, and Sushkov, and, ad-

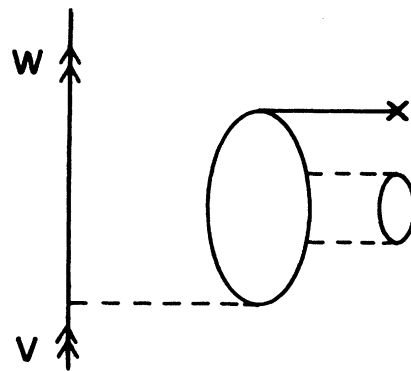


FIG. 15. Sample fourth-order contributions to the matrix element containing a triple excitation.

TABLE IV. Effect of rescaling of valence single-excitation coefficients on hyperfine constants (hfs) and electric dipole transition-matrix elements ( $E1$ ). The table shows the % discrepancy from experiment with and without rescaling.

State		$\Delta\pm\Delta^{\text{expt}}$ (%) (No rescaling)	$\Delta\pm\Delta^{\text{expt}}$ (%) (Rescaled)
6s	hfs	-0.31±0.00	0.58±0.00
7s	hfs	-0.34±0.00	0.34±0.00
6p <sub>1/2</sub>	hfs	0.27±0.04	1.18±0.04
7p <sub>1/2</sub>	hfs	-0.15±0.04	0.72±0.04
8p <sub>1/2</sub>	hfs	-0.43±0.23	0.38±0.23
6p <sub>3/2</sub>	hfs	-0.97±0.12	-0.18±0.12
7p <sub>3/2</sub>	hfs	-2.11±0.36	-1.12±0.36
8p <sub>3/2</sub>	hfs	-1.75±0.13	-0.81±0.13
6s-6p <sub>1/2</sub>	E1	0.11±0.22	-0.23±0.22
6s-7p <sub>1/2</sub>	E1	-1.74±0.70	-1.40±0.70
6s-6p <sub>3/2</sub>	E1	0.15±0.16	-0.20±0.16
6s-7p <sub>3/2</sub>	E1	-1.38±1.72	-1.13±1.72
7s-6p <sub>1/2</sub>	E1	-0.15±0.52	0.04±0.52
7s-7p <sub>1/2</sub>	E1	1.19±0.20	0.77±0.20
7s-6p <sub>3/2</sub>	E1	-0.45±0.46	-0.15±0.46
7s-7p <sub>3/2</sub>	E1	1.25±0.14	0.80±0.14

ditionally, ladder diagrams and effects associated with the interaction between the valence electron and the core. In the third order, these additional effects amount to -1.2% for the 6s removal energy; we find that, after iteration to all orders in the manner described in Sec. II, the net contribution of these terms is still of order 1%. On the other hand, the approach of Dzuba, Flambaum, and Sushkov implicitly contains the most important nonlinear contributions, which have been omitted entirely here. Both calculations neglect effects associated with triple excitations. Dzuba, Flambaum, and Sushkov re-

port accuracies slightly better than those obtained here, but in view of the terms omitted in their calculation, this would appear to be fortuitous.

As a next step, we plan to incorporate the most important terms missed in the present work, specifically, the nonlinear terms associated with single and double excitations, and certain classes of triple excitations. The inclusion of nonlinear terms is straightforward and well documented,<sup>1</sup> and leads to the full coupled-cluster equations for single and double (CCSD) excitations. Several nonrelativistic numerical implementations of CCSD exist for molecules, and one has been developed specifically for atoms by Lindgren and collaborators (see, e.g., Refs. 1 and 17). Our proposed implementation would be relativistic, an extension of the procedure outlined in Sec. II. As mentioned in Secs. II and IV, the explicit introduction of triple excitations leads to excessive requirements on storage for the basis sets and numbers of channels we would prefer to use for calculations of parity nonconservation. Thus we propose to handle triple excitations approximately in terms of the modifications to the single- and double-excitation equations given in Eqs. (16) and (17). We have implemented the single-excitation modification in the present work; in the next stage we propose to implement also the modification to the double-excitation equation. This would enable us to pick up the terms in Fig. 14 and 15. At this stage the valence removal energy would in fact be complete through fourth order. We think that CCSD excitations augmented by the set of triple excitations discussed above offers hope of a practical relativistic scheme capable of predicting removal energies and matrix elements in cesium at the tenth of a percent level.

#### ACKNOWLEDGMENTS

We would like to acknowledge helpful conversations with Ingvar Lindgren. This research was supported in part by National Science Foundation Grant No. PHY89-07258. The calculations were carried out on the National Center for Supercomputing Applications CRAY-2.

\*Present address: University of California, Department of Physics, L-402, Lawrence Livermore National Laboratory, P.O. Box 808, Livermore, CA 94550.

<sup>1</sup>I. Lindgren and J. Morrison, *Atomic Many-Body Theory*, 2nd ed. (Springer-Verlag, Berlin, 1986).

<sup>2</sup>S. A. Blundell, W. R. Johnson, and J. Sapirstein, *Phys. Rev. A* **37**, 2764 (1988); **38**, 2699 (1988); **42**, 1087 (1990).

<sup>3</sup>R. F. Bishop and H. G. Kümmel, *Phys. Today* **40** (3), 52 (1987).

<sup>4</sup>S. A. Blundell, W. R. Johnson, and J. Sapirstein, *Phys. Rev. Lett.* **65**, 1411 (1990).

<sup>5</sup>V. A. Dzuba, V. V. Flambaum, P. G. Silvestrov, and O. P. Sushkov, *Phys. Lett. A* **141**, 147 (1989); A. C. Hartley, E. Lindroth, and A.-M. Mårtensson-Pendrill, *J. Phys. B* **23**, 3417 (1990).

<sup>6</sup>M. A. Bouchiat and C. Bouchiat, *J. Phys. (Paris)* **35**, 899 (1974).

<sup>7</sup>S. A. Blundell, W. R. Johnson, and J. Sapirstein, *Phys. Rev. A* **40**, 2233 (1989).

<sup>8</sup>S. A. Blundell, W. R. Johnson, and J. Sapirstein, *Phys. Rev. A* **38**, 4961 (1988).

<sup>9</sup>S. A. Blundell, W. R. Johnson, and J. Sapirstein, *Phys. Rev. A* **42**, 3751 (1990).

<sup>10</sup>I. Lindgren, *J. Phys. B* (to be published).

<sup>11</sup>J. Sucher, *Int. J. Quantum Chem.* **24**, 3 (1984).

<sup>12</sup>W. R. Johnson, M. Idrees, and J. Sapirstein, *Phys. Rev. A* **35**, 3218 (1987).

<sup>13</sup>V. A. Dzuba, V. V. Flambaum, and O. P. Sushkov, *Phys. Lett.* **142**, 373 (1989).

<sup>14</sup>I. Lindgren, *Int. J. Quantum Chem. S* **12**, 33 (1978).

<sup>15</sup>R. J. Bartlett, in *Many-Body Methods in Quantum Chemistry*, Vol. 52 of *Springer Lecture Notes in Quantum Chemistry*, edited by U. Kaldor (Springer-Verlag, Berlin, 1989).

<sup>16</sup>S. A. Blundell, W. R. Johnson, and J. Sapirstein, *Phys. Rev. A* **37**, 307 (1988).

<sup>17</sup>S. Salomonson and A. Ynnerman (unpublished).